JOURNAL OF Materials CHEMISTRY

# Zirconia thin films by atomic layer epitaxy. A comparative study on the use of novel precursors with ozone

**Matti Putkonen and Lauri Niinistö**

*Laboratory of Inorganic and Analytical Chemistry, Helsinki University of Technology, P.O Box 6100, FIN-02015 Espoo, Finland. E-mail: Lauri.Niinisto@hut.fi*

***Received 15th June 2001, Accepted 24th August 2001***
***First published as an Advance Article on the web 11th October 2001***

Zirconium oxide thin films have been deposited by atomic layer epitaxy (ALE) using $Zr(thd)_4$, $Cp_2Zr(CH_3)_2$ and $Cp_2ZrCl_2$ (thd = 3,3,5,5-tetramethylheptane-3,5-dionate, Cp = cyclopentadienyl) as zirconium precursors and ozone as the oxygen source. A plateau of constant growth rate (ALE window) was observed for the $Zr(thd)_4/O_3$ process at 375–400 °C, for $Cp_2Zr(CH_3)_2/O_3$ at 310–365 °C and for $Cp_2ZrCl_2/O_3$ at 275–350 °C. Within these temperature ranges constant deposition rates of 0.24, 0.55 and 0.53 Å (cycle)$^{-1}$ were obtained, respectively. Deposited films were characterised by XRD and AFM for crystallinity and surface morphology, while TOF-ERDA was used to analyse the $ZrO_2$ film stoichiometry and possible impurities. Films deposited by optimised parameters from $Cp_2Zr(CH_3)_2/O_3$ and $Cp_2ZrCl_2/O_3$ were crystalline showing the preferred (−111) orientation of monoclinic $ZrO_2$. In all films, the orthorhombic zirconia phase was also present, although at higher temperatures its relative amount decreased. $Zr(thd)_4/O_3$ process produced films with lowest crystallinity consisting of both orthorhombic and monoclinic phases. According to TOF-ERDA, films were nearly stoichiometric with less than 0.5 atom% hydrogen and carbon. Outside the ALE window, a small chlorine contamination (0.1–0.3 wt%) was observed by XRF when the $ZrO_2$ films were deposited from $Cp_2ZrCl_2/O_3$ at 200–275 °C.

## Introduction

Zirconium dioxide is a thermally and chemically stable material used for optical and electrical applications. For example, $ZrO_2$ has attracted interest as mirrors and antireflective coatings, thermal barriers and hard protective layers.[1–5] Due to its high permittivity ($\varepsilon = 17$–$22$),[6,7] $ZrO_2$ thin films have also been used as dielectrics in microelectronics.[8,9] The use of $ZrO_2$ as a buffer layer for high $T_c$-superconductors[10] and high temperature insulating shields[11] has also been studied. Preparation of complex dielectric films containing zirconium, such as $ZrTiO_4$,[12] has been reported as well.

$ZrO_2$ has three different structural polymorphs, of which the monoclinic (M) phase is the thermodynamically stable one at room temperature. High temperature forms of $ZrO_2$, namely the cubic (C) and tetragonal (T) polymorphs, can be stabilised at room temperature by several ways. The mechanism of phase transformation has frequently been studied and different routes have been suggested.[13,14] Physical properties, such as strain, film thickness and crystallite size, affect the stabilisation and phase transformation of $ZrO_2$. The cubic form of $ZrO_2$ is usually stabilized in thin films by adding other oxides, typically $Y_2O_3$,[15] but also $Sc_2O_3$,[16] CaO,[17] $CeO_2$,[18–20] $In_2O_3$,[21] $Gd_2O_3$,[15] MgO,[15,17] $Al_2O_3$ [16,22] and $MgAl_2O_4$ [23] have been used. Yttria stabilised zirconium oxide (YSZ),[24–26] has been used as a buffer layer for high-$T_c$ superconducting films as such or together with $CeO_2$ or $Y_2O_3$,[27–29] as well as in solid electrolyte applications for oxygen pumps,[30] sensors[31] and catalysts.[19] Furthermore, relatively thick (> 2 μm), stabilised $ZrO_2$ films have been utilised in solid-oxide fuel cells[32] and oxygen membranes.[33] Other than yttrium stabilised $ZrO_2$ compounds have been suggested for certain applications, for example, in high temperature[22] and corrosion protection layers[18] as well as in transparent conductive oxides.[21] $ZrO_2$ is also a constituent of several interesting oxide thin films of complex composition, such as $Pb(Zr,Ti)O_3$ [34,35] and $Pb(Zr,Ti,Nb)O_3$.[35] The application potential of these ferroelectric oxides has been studied for capacitors in integrated circuits for dynamic random access (DRAMs) and non-volatile memories.[36]

Atomic layer epitaxy (ALE),[37] also referred to as atomic layer deposition (ALD) or atomic layer CVD (ALCVD), has been successfully employed for the deposition of a variety of oxide films.[38–40] It is based on alternating saturative reactions on the substrate surface, which makes the thin film growth process self-limiting and easy to control.[41] ALE has been used for the deposition of amorphous and nanocrystalline $ZrO_2$ films from zirconium tetrachloride[42] and $ZrO[C(CH_3)_3]_4$,[43] respectively. $ZrO_2$ thin films were deposited at 500 °C from $ZrCl_4/H_2O$ precursors but more recently the depositions have also been successfully carried out at a much lower temperature, *viz.* 300 °C.[44,45] Furthermore, the ALE deposition of $ZrO_2$ for catalyst preparation and surface-controlled precursor chemisorption has been studied on high surface area silica substrates with $ZrCl_4$ [46] and $Cp_2ZrCl_2$ [47] precursors, respectively, in an attempt to quantitatively establish the stoichiometry and mechanism of the surface reactions.

ALE/ALD can be compared to the other major chemical deposition method, *viz.* CVD which has frequently been used for the deposition of $ZrO_2$. Different types of precursors have been utilised in the CVD depositions of $ZrO_2$ including pure inorganics,[42,48,49] β-diketonates[2,25,50] and alkoxides[51,52] as well as mixed-ligand[53–55] and amido complex[56] compounds of zirconium. In addition, the CVD deposition of $ZrO_2$ has been reported from volatile organo-zirconium compounds,[1] including $Cp_2Zr(CH_3)_2$.[57] According to the best of our knowledge, $Cp_2ZrCl_2$ has not yet been used as a precursor in CVD processes. However, it is a sufficiently volatile compound with thermal stability up to 500 °C.[58]

Generally speaking, precursors similar to those used in CVD are also applicable to an ALE process provided that certain requirements, such as thermal stability and sufficiently high reactivity, are met. The properties of different types of ALE precursors have recently been discussed.[59] Typically, β-diketonate and inorganic compounds have been employed as

ALE precursors, but interest towards deposition of oxide thin films also from true organometallic compounds has increased, because lower deposition temperatures and higher rates can be achieved. For example, ALE processes utilizing organometallic precursors for $Al_2O_3$,[60] MgO,[61] $BaTiO_3$ [62] and $SrTiO_3$ [62] have recently been developed. In this paper we report the results of $ZrO_2$ deposition by atomic layer epitaxy using organometallic compounds, namely $Cp_2Zr(CH_3)_2$ and $Cp_2ZrCl_2$. For comparison, we report the results of $ZrO_2$ film depositions from a β-diketonate type precursor, $Zr(thd)_4$. In all cases ozone was used as the oxygen source.

## Experimental

Commercial $Cp_2ZrCl_2$ (Strem Chemicals, #93-4002, 99%) (Cp = cyclopentadienyl, $C_5H_5$) was used without purification while the two other zirconium precursors were synthesised by published methods. Thus, $Cp_2Zr(CH_3)_2$ was synthesised by the method described by Samuel and Rausch[63] while $Zr(thd)_4$ (thd = 2,2,6,6-tetramethylheptane-3,5-dionate) was prepared according to Morozova *et al.*[64] After the synthesis, the precursors were purified by sublimation and their volatility was checked by simultaneous TG/DTA in a Seiko SSC 5200 thermobalance. 2 mbar pressure and nitrogen (99.999%) carrier gas were used in order to simulate the ALE deposition conditions.[65]

Zirconium oxide thin films were deposited in a commercial flow-type hot-wall atomic layer epitaxy (ALE) reactor (F-120 by ASM Microchemistry Ltd.) using $Zr(thd)_4$, $Cp_2Zr(CH_3)_2$ and $Cp_2ZrCl_2$ as zirconium precursors and ozone as oxidising agent. $O_3$ was generated from $O_2$ (99.999%) in an ozone generator (Fischer model 502). Nitrogen (>99.999%, Schmidlin UHPN 3000 $N_2$ generator) was used as a carrier and purging gas. Thin film depositions were carried out under a 2–3 mbar pressure onto (100) oriented silicon and soda lime glass substrates measuring $10 \times 5$ cm$^2$. All substrates used were cleaned ultrasonically in ethanol and water before use. Zirconium precursors were evaporated from open glass crucibles. The deposition rate of $ZrO_2$ was studied as a function of the deposition temperature at 275–500 °C ($Zr(thd)_4/O_3$), 250–500 °C ($Cp_2Zr(CH_3)_2/O_3$) and 200–500 °C ($Cp_2ZrCl_2/O_3$).

Reflectance and transmittance spectra were measured in a Hitachi U-2000 double beam spectrophotometer. Thicknesses of the deposited films were calculated by the optical fitting method described by Ylilammi and Ranta-aho.[66] Crystallite orientations and crystallinity of the deposited films were determined by X-ray diffraction using Cu Kα radiation in a Philips MPD 1880 diffractometer. Surface morphology was studied by a Nanoscope III atomic force microscope (Digital Instruments) operated in tapping mode. Samples were measured with a scanning frequency of 1–2 Hz. Several wide scans (10–20 μm) were performed from different parts of samples to check the uniformity of the sample. Final images were measured from a scanning area of $2 \times 2$ μm. Roughness values were calculated as root mean square values (rms).

Impurity levels were analysed by X-ray fluorescence (XRF) and time-of-flight elastic recoil detection analysis (TOF-ERDA). Chlorine impurities in the samples were measured by a Philips PW 1480 WDS X-ray spectrometer equipped with a Rh anode. The chlorine impurity levels were then quantitatively estimated using the Uniquant 4.34 program (Omega Data Systems, Netherlands), which is based on fundamental parameters and experimentally determined instrumental sensitivity factors.[67]

TOF-ERDA measurements for other impurities than chlorine and for the Zr/O ratio were carried out at the Accelerator Laboratory of the University of Helsinki. In this method[68] heavy ions are projected into the sample and the signal consists of forward recoiling sample atoms ejected by the ion beam. Both velocity and energy for recoiled atoms were determined using timing gates and a charged particle detector, which enables the differentiation of different masses. With known stopping power and scattering cross sections, elemental depth distributions can also be calculated. For these TOF-ERDA studies, a 53 MeV $^{127}I^{10+}$ ion beam was used, obtained from a 5 MV tandem accelerator EGP-10-II. Samples were measured at 20° tilt and the recoils were detected at 40°, with respect to the incoming beam. For heavy recoil, energy spectra were obtained from the TOF signals and hydrogen spectra from the charged particle detector. In TOF ERD analysis the uncertainties of the impurity contents are due to statistical and possible systematic errors on the stopping powers. The uncertainties fall below 0.1 atom% units for contents below 1 atom% and below 0.2 atom% for contents above 1 atom%.

## Results and discussion

### Precursor analysis and $ZrO_2$ film growth

Precursors were analysed by TG/DTA which indicated a complete volatility except in the case of $Cp_2Zr(CH_3)_2$ where a few percent residue was left unvolatilised (Fig. 1). Onset values for volatilisation at 2–3 mbar pressure were 200–205 °C for $Zr(thd)_4$, 100–105 °C for $Cp_2Zr(CH_3)_2$ and 155–160 °C for $Cp_2ZrCl_2$. As we were unable to transfer the samples in a completely inert atmosphere into the TG/DTA apparatus, a slight decomposition of $Cp_2Zr(CH_3)_2$ was observed. For this particular precursor the amount of the weight loss at 170–190 °C and the amount of sublimation residue increased when samples were stored for longer periods in ambient atmosphere. Finally, after 60 hours of storing, no weight loss due to original $Cp_2Zr(CH_3)_2$ was detected. However, when $Cp_2Zr(CH_3)_2$ was transferred inertly into the ALE reactor, a complete volatility was observed. According to DTA results, no melting of the precursors took place before sublimation. Source material temperatures for the ALE depositions were estimated from the TG results. Thus, $Zr(thd)_4$, $Cp_2Zr(CH_3)_2$ and $Cp_2ZrCl_2$ were evaporated from open crucibles kept at 170, 70 and 140 °C, respectively.

The deposition rate of $ZrO_2$ as a function of deposition temperature was studied with different precursors. Pulse times for reactants were kept constant and sufficiently long in order to obtain a complete surface saturation on the substrate. Precursor pulse times were 0.8–1.0 s depending on the precursor selected; the ozone pulse time was kept constant at 1.5 s. Purge times of 1.0–3.0 s between reactive pulses were compared but no differences in growth rates were observed and therefore 1 s was chosen for all experiments. A plateau in the growth rate was observed for each of the precursors. As expected, the observed growth rate with $Zr(thd)_4/O_3$ was low due to the bulky size of the precursor. Previously in CVD

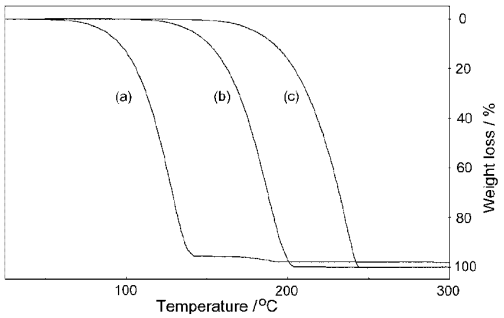


**Fig. 1** TG curves of the precursors used; $Cp_2Zr(CH_3)_2$ (a), $Cp_2ZrCl_2$ (b) and $Zr(thd)_4$ (c). Heating rate was 10 °C min$^{-1}$ and sample weight ~10 mg. This measuring pressure was 2 mbar.

experiments[50] observed high thermal stability of $Zr(thd)_4$ was the probable reason for the unusually high deposition temperature required as compared to the other ALE processes based on β-diketonate precursors and ozone.[38] A constant growth rate of 0.24 Å (cycle)$^{-1}$ was obtained in a narrow temperature range of 375–400 °C (Fig. 2). A slightly lower growth rate (0.22 Å (cycle)$^{-1}$) was observed at 350 °C. At still lower temperatures the growth rate slowly decreased down to 0.08 Å (cycle)$^{-1}$, which was the value obtained at 275 °C. When the deposition temperature was increased above the plateau region up to 500 °C, the growth rate increased significantly to 0.41 Å (cycle)$^{-1}$, but at the same time the thickness profile at the leading edge of the films increased, indicating precursor decomposition. This is a typical phenomenon in the ALE deposition of oxides, although the heavier Group 3 β-diketonates (*e.g.* the rare earths) appear to produce uniform films also above the ALE window.[69,70] Likewise, uniform $ZrO_2$ films can be deposited by CVD from $Zr(thd)_4$ at 540–575 °C,[50] which is about 150–200 °C higher than the temperature used in the present ALE depositions.

$ZrO_2$ thin films deposited from $Cp_2Zr(CH_3)_2/O_3$ were uniform when prepared below 365 °C and a constant growth rate of 0.55 Å (cycle)$^{-1}$ was obtained in the region of 310–365 °C (Fig. 2). Below this, the deposition rate decreased to 0.22 Å (cycle)$^{-1}$, obtained at 250 °C. The maximum growth rate of 1.04 Å (cycle)$^{-1}$ was reached at 500 °C. Unlike the other two precursors, where the growth rate increases only slightly above the constant growth rate plateau, there was for the $Cp_2Zr(CH_3)_2/O_3$ process a sudden increase in the growth rate and thickness profile above 365 °C. For comparison, it can be noted that CVD depositions from $Cp_2Zr(CH_3)_2$ have been performed at 400–550 °C, although it has also been possible to carry out depositions at 300 °C in the presence of $O_2/H_2O$ producing $ZrO_2$ films with, however, 5% carbon.[57]

$ZrO_2$ films were prepared from $Cp_2ZrCl_2/O_3$ in a similar manner. Below 400 °C the deposited films were uniform with only a minor thickness profile within the substrate length of 10 cm. A constant growth rate of 0.53 Å (cycle)$^{-1}$ was observed at 275–350 °C (Fig. 2). Above 350 °C the growth rate slowly increased with increasing temperature. Maximum growth rate of 0.64 Å (cycle)$^{-1}$ was obtained at 500 °C, measured 2 cm from the leading edge of the substrate. Compared to the depositions performed on high surface area silica,[47] where uniform samples were obtained at 300–350 °C, controlled thin film deposition appears to occur here over a slightly wider temperature region. This may be due to different experimental conditions, mainly pressure.

Existence of an ALE window, *i.e.* temperature region where the deposition is surface-controlled, was checked for each process by increasing the reactive pulsing times (Fig. 3). Both

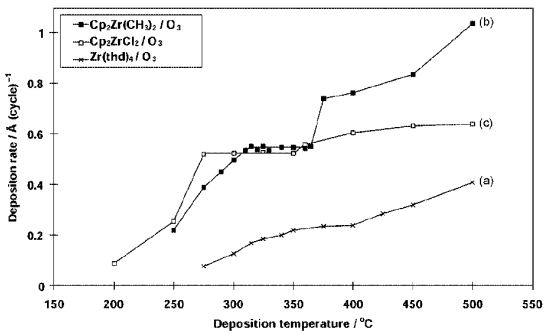


**Fig. 2** Deposition rate of $ZrO_2$ thin films as a function of the deposition temperature from $Zr(thd)_4/O_3$ (a), $Cp_2Zr(CH_3)_2/O_3$ (b) and $Cp_2ZrCl_2/O_3$ (c). Pulsing times were 0.8 and 2.0 s for the Zr precursors used and ozone, respectively.

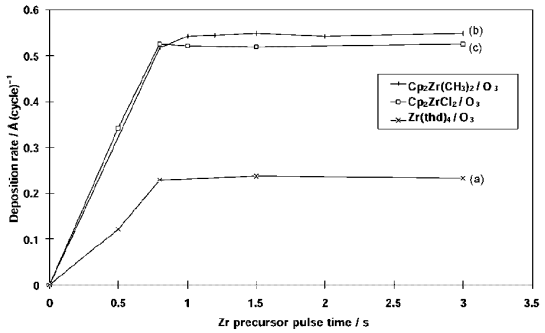


**Fig. 3** Deposition rates of $ZrO_2$ thin films as a function of Zr precursor pulsing times. Deposition temperatures were 375 °C ($Zr(thd)_4/O_3$) (a), 350 °C ($Cp_2Zr(CH_3)_2/O_3$) (b) and 300 °C ($Cp_2ZrCl_2/O_3$) (c). Pulsing time was 2.0 s for $O_3$ and purging times 1.5–2.0 s depending on the Zr precursor pulsing time.

$Zr(thd)_4/O_3$ and $Cp_2ZrCl_2/O_3$ processes produced uniform films when precursor pulsing times were 0.8–3.0 s at 375 and 300 °C, respectively. A slightly longer pulsing time (1.0 s) was needed to obtain a complete surface saturation in the $Cp_2Zr(CH_3)_2/O_3$ process at 350 °C. Regardless of the process used, ozone pulse times of 1.5–3.5 s resulted in uniform films. Another characteristic and beneficial feature of an ALE-type process is the facile control of the film thickness by the number of deposition cycles. A linear dependency was obtained when $ZrO_2$ was deposited by optimised pulsing parameters (Fig. 4).

### Characterisation of the $ZrO_2$ films

$ZrO_2$ films from the $Zr(thd)_4/O_3$ process were only slightly crystalline regardless of the deposition temperature and the substrate used. Broad diffraction peaks (FWHM values 0.5–0.65° 2$\theta$ of M(002) peak on Si(100) substrate) also indicated low crystallinity, which together with the several structural polymorphs of $ZrO_2$ complicates an interpretation of the diffraction diagrams. Thus, a straightforward identification of all peaks was not possible because of the monoclinic (200) and orthorhombic (O) (002) reflections overlapping at a *d*-value of 2.62 Å. The strongest peak, albeit still low in intensity, was identified as belonging either to the M(200) or O(002) reflection and was observed in films deposited at 300–500 °C (Fig. 5a, d). Very low intensity M(−221) and M(−203) reflections were also observed in all samples. Regardless of the deposition temperature, a reflection at $d$=2.96 Å, identified as O(111), was also observed. The intensities of the M(−111) and O(111) reflections increased only slightly when the deposition temperature was increased (Fig. 6a).

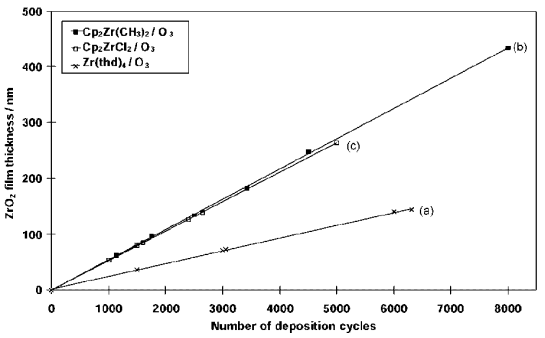


**Fig. 4** $ZrO_2$ thin film thickness as a function of number of deposition cycles. Deposition temperatures were 375 °C ($Zr(thd)_4/O_3$) (a), 350 °C ($Cp_2Zr(CH_3)_2/O_3$) (b) and 300 °C ($Cp_2ZrCl_2/O_3$) (c). Pulsing times were 0.8–1.0 s for zirconium precursors and 2.0 s for $O_3$.

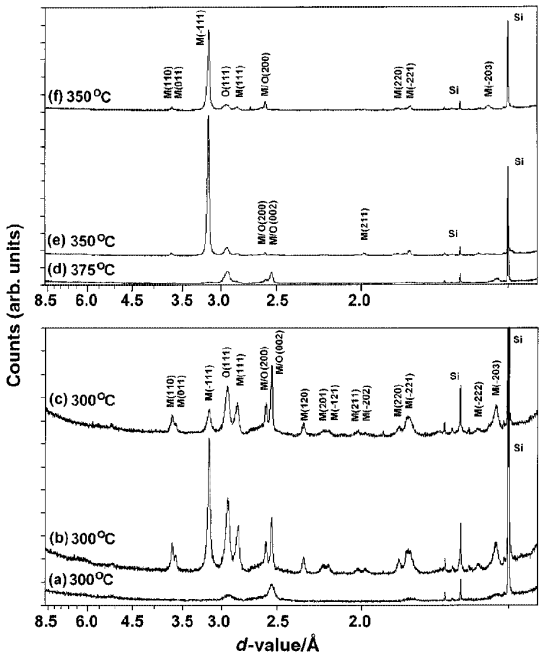


**Fig. 5** X-Ray diffraction patterns of the $ZrO_2$ films deposited from $Zr(thd)_4/O_3$ (a, d), $Cp_2Zr(CH_3)_2/O_3$ (b, e) and $Cp_2ZrCl_2/O_3$ (c, f). Si(100) was used as a substrate. Diffraction peaks were identified according to JCPDS reference values (cards 37-1413 and 37-1484 for orthorhombic (O) and monoclinic (M) phases, respectively). M/O(002) notation corresponds to overlapping M(200) and O(002) reflections.

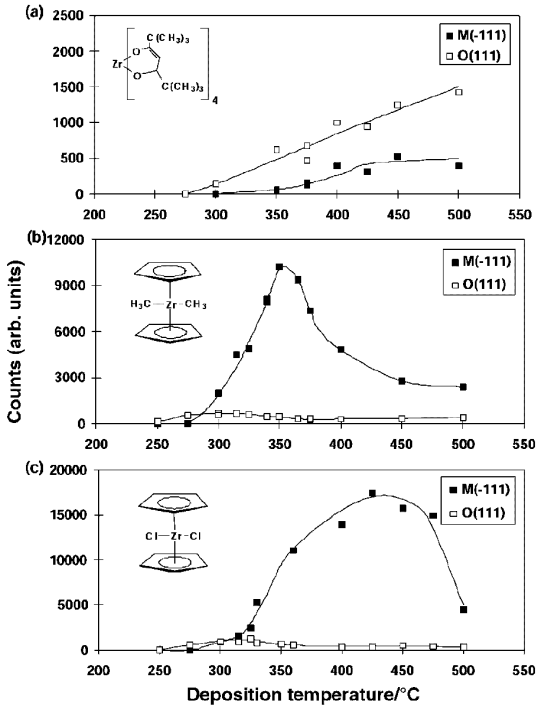


**Fig. 6** XRD peak intensities of monoclinic (−111) and orthorhombic (111) reflections of the deposited $ZrO_2$ thin films onto Si(100). Depositions were carried out from $Zr(thd)_4/O_3$ (a), $Cp_2Zr(CH_3)_2/O_3$ (b) and $Cp_2ZrCl_2/O_3$ (c). Si(100) was used as substrate. Film thicknesses were 130–170 nm.

Depositions carried out by the $Cp_2Zr(CH_3)_2/O_3$ process resulted in weakly crystalline $ZrO_2$ films when deposited below 300 °C; the M(−111) reflection was barely observable. M(−111) became the most intense reflection in films deposited at 300 °C, but several other peaks were identified as well, when films were deposited onto Si(100) (Fig. 5b). At higher deposition temperatures, the intensity of the M(−111) orientation increased rapidly, exhibiting a maximum value at 350 °C (Fig. 6b). The weaker O(111) reflection was observed to be present in the whole temperature range of 250–500 °C. Generally, the film crystallinity decreased when deposition temperature was increased above 350 °C, however, FWHM value of the M(111) reflection was in the range of 0.25–0.30° $2\theta$, and a certain minimum value was seen in films deposited at 350 °C.

The third process, *i.e.* that based on $Cp_2ZrCl_2/O_3$, produced slightly crystalline $ZrO_2$ with monoclinic and orthorhombic phases at lower temperatures (250–300 °C). By increasing the deposition temperature the crystallinity of the films deposited onto Si(100) could be enhanced, thus producing almost completely (−111) oriented monoclinic $ZrO_2$ films above 350 °C (Figs. 5c, f and 6c). The O(111) reflection was also observed in the crystalline films (275–500 °C) being strongest in films deposited around 300 °C (Fig. 6c). Maximum crystallinity was observed in films deposited around 425–450 °C. Measured M(111) peak widths expressed in terms of FWHM values were in the range of 0.25–0.35° $2\theta$, exact values depending on the deposition temperature.

In the present study, in addition to the monoclinic phase an orthorhombic phase was also observed regardless of the zirconium precursor used. Typically while the tetragonal and monoclinic phases have been observed in CVD-deposited thin films, the metastable orthorhombic phase of $ZrO_2$ has been only seldom reported in thin films[71] and in bulk material only when the grain size is very fine (below 30 nm).[72] Recently, ALE-deposited nanocrystalline films from various precursors have been identified as being either monoclinic or metastable tetragonal $ZrO_2$, but not orthorhombic.[43]

Stoichiometry and impurity levels of $ZrO_2$ films were examined by TOF-ERDA from films deposited onto Si(100) substrates within the ALE window of each process. The zirconium to oxygen ratio was nearly stoichiometric (Table 1) but a slight excess of oxygen of the order of a few percent was observed regardless of the precursor used. Carbon and hydrogen impurity levels were quite low in each case. Fluorine content was around 0.1 atom% regardless of the precursor used. This is probably a contamination caused by the materials used in the reactor set-up with Teflon gaskets and perfluorinated vacuum greases. In addition, possible chlorine impurities

**Table 1** Stoichiometry and impurity levels of the $ZrO_2$ thin films deposited from different precursors onto Si(100) substrates analysed by TOF-ERDA

| Process | Deposition temperature/ °C | Zr : O ratio | Carbon/atom% | Hydrogen/atom% | Fluorine/atom% |
|---|---|---|---|---|---|
| $Zr(thd)_4/O_3$ | 375 | 0.46 ± 0.03 | 0.20 | 0.3 | < 0.1 |
| $Cp_2ZrCl_2/O_3$ | 300 | 0.47 ± 0.03 | 0.54 | 0.5 | 0.1 |
| $Cp_2Zr(CH_3)_2/O_3$ | 315 | 0.48 ± 0.03 | 0.16 | 0.1 | 0.1 |

in $ZrO_2$ films originating from $Cp_2ZrCl_2/O_3$ were studied by XRF. In earlier studies, it has been observed that at lower temperatures, ALE deposition of oxide materials from chlorine-containing precursors may lead to Cl impurities being incorporated into the deposited films. For example, chlorine contaminations in other Group 4 oxide films, namely $TiO_2$ and $HfO_2$, have been observed when deposited from $TiCl_4/H_2O$ [73] and $HfCl_2/H_2O$,[74] respectively. However, no similar data are available in the literature for low temperature deposition from $ZrCl_4/H_2O$ precursors. We found that chlorine from $Cp_2ZrCl_2/O_3$ was not incorporated into the $ZrO_2$ films when they were deposited above 275 °C. However, below 275 °C, 0.1–0.3 wt% Cl was observed depending on the deposition temperature. According to TOF-ERDA results, chlorine content was below the detection limit (0.07 atom%) when $ZrO_2$ films were deposited at 300 °C or above.

$ZrO_2$ film surface morphology was analysed by AFM as a function of the deposition temperature and film thickness (Fig. 7). In the first set of samples, the thickness of the films was kept at 100–140 nm while the deposition temperature was varied. When the $Zr(thd)_4/O_3$ process was used, the $ZrO_2$ film roughness increased from 1.7 to 5.3 nm with increasing deposition temperature from 315 to 450 °C. On the other hand, the roughness of $ZrO_2$ films was quite constant, 2.8–3.3 nm, when deposited by the $Cp_2Zr(CH_3)_2/O_3$ process at 275–400 °C. However, the roughness increased when the deposition temperature was increased above 400 °C. The third process, *i.e.* that based on $Cp_2ZrCl_2/O_3$, produced $ZrO_2$ films with roughness of 3.0–5.0 nm when deposited at 275–450 °C. A second set of samples with different thicknesses of 40–400 nm was deposited by the $Zr(thd)_4/O_3$ process at 375 °C, by $Cp_2Zr(CH_3)_2/O_3$ at 350 °C and by $Cp_2ZrCl_2/O_3$ at 300 °C and an increase in the roughness was observed regardless of the process used (Fig. 8). However, compared to previous $ZrO_2$ depositions by ALE using $ZrCl_4$ and $H_2O$ as precursors,[42] where agglomeration of the films was observed, increases in roughness and grain size were much smaller. This indicates, as expected, that ALE deposition of $ZrO_2$ using β-diketonate or organometallic precursors proceeds by a different mechanism from that observed with $ZrCl_4$ as a precursor.

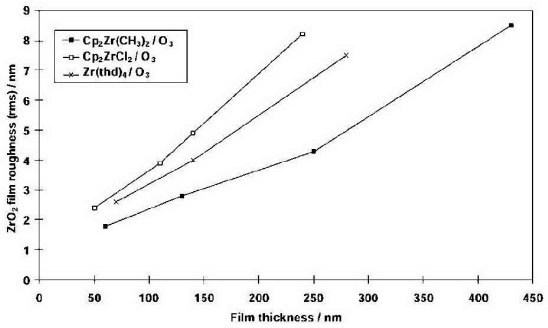


**Fig. 8** Roughness of the $ZrO_2$ films on Si(100) substrates as a function of the film thickness measured by AFM. The film deposition temperature was 375 °C for $Zr(thd)_4/O_3$, 350 °C for $Cp_2Zr(CH_3)_2/O_3$ and 300 °C for $Cp_2ZrCl_2/O_3$.

## Conclusions

ALE deposition of $ZrO_2$ thin films was successfully performed from organometallic and β-diketonate type precursors using ozone as oxidizer. A surface-controlled deposition region (ALE window) was observed for the $Zr(thd)_4/O_3$ process at 375–400 °C and for $Cp_2Zr(CH_3)_2/O_3$ at 310–365 °C while this was at 275–350 °C for the $Cp_2ZrCl_2/O_3$ system. Constant growth rates of 0.24, 0.55 and 0.53 Å (cycle)$^{-1}$, respectively, were measured for these processes. Saturation of growth rate as a function of reactive pulses together with a linear dependency of film thickness as a function of the number of deposition cycles indicate a controlled ALE-type growth which enables a straightforward control of the deposition process.

The crystallinity of the $ZrO_2$ films depends on the precursors used as well as on the deposition temperature. Low

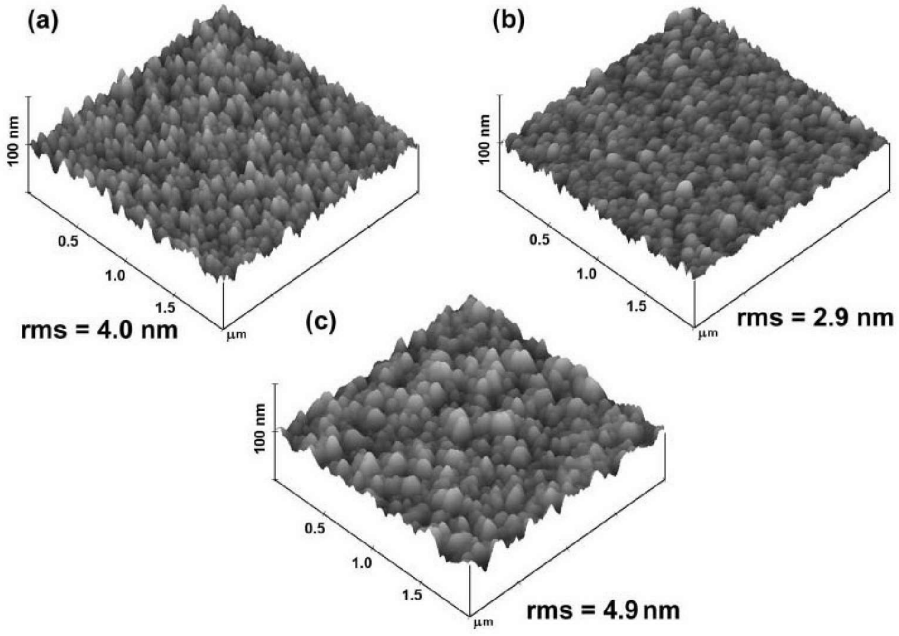


**Fig. 7** AFM images of $ZrO_2$ films deposited onto Si(100) substrates (a) by $Zr(thd)_4/O_3$ at 375 °C, (b) by $Cp_2Zr(CH_3)_2/O_3$ at 350 °C and (c) by $Cp_2ZrCl_2/O_3$ at 300 °C. Film thickness was 130–140 nm. Depth scale: 50 nm from black to white.

temperature depositions resulted in films with low crystallinity containing both the orthorhombic and monoclinic phases. For each precursor, as expected, the crystallinity increased with increasing deposition temperature. The $Zr(thd)_4/O_3$ process produced films with the lowest crystallinity. The orientation and crystallinity of the films deposited from $Cp_2ZrCl_2/O_3$ and $Cp_2Zr(CH_3)_2/O_3$ were quite similar. However, $ZrO_2$ films deposited from $Cp_2Zr(CH_3)_2/O_3$ exhibited maximum crystallinity at a 75–100 °C lower temperature than films deposited by the $Cp_2ZrCl_2/O_3$ process. In the latter case, maximum values were obtained above the ALE window, whereas films of highest crystallinity were obtained from the $Cp_2Zr(CH_3)_2/O_3$ precursors when deposited within the ALE window.

AFM results indicate that the $ZrO_2$ film roughness was dependent on the deposition temperature when deposited by the $Zr(thd)_4/O_3$ process. The rms roughness of 100–140 nm thick films remained quite constant (2.8–4 nm) when $Cp_2Zr(CH_3)_2$ or $Cp_2ZrCl_2$ were used as zirconium precursors. An increase in roughness as function of film thickness was observed regardless of the process used.

According to TOF-ERDA results, nearly stoichiometric films were obtained in all cases. Impurity levels were dependent on the selected precursor but they were quite low in each case, *i.e.* 0.1–0.5 and 0.2–0.5 atom% for H and C, respectively. $ZrO_2$ films deposited from $Cp_2ZrCl_2/O_3$ below the ALE window contained chlorine as an impurity. According to XRF data the chlorine content decreased with increasing temperature being 0.3 wt% at 200 °C and 0.1 wt% at 275 °C. At 300 °C chlorine was no longer detected by TOF-ERD analysis.

The present study clearly demonstrates the suitability of novel precursors, previously used only in CVD, also for ALE depositions of $ZrO_2$ thin films. For future applications, volatile organometallic precursors seem to outperform the conventional volatile β-diketonate complexes. Although in the case of zirconium the growth rates obtained with $Cp_2ZrCl_2/O_3$ and $Cp_2Zr(CH_3)_2/O_3$ were comparable to the conventional $ZrCl_4/H_2O$ process, the better crystallinity may be advantageous in some applications. The level of chlorine and other residues remaining in the films depend on the selected process and its parameters but the impurity level was generally low. Thus, from the wide range of ALE processes now available for the processing of $ZrO_2$ thin films it is possible to choose the optimum one for $ZrO_2$-containing thin film materials depending on the application aimed at.

## Acknowledgements

We wish to thank Prof. P. Hautojärvi, Laboratory of Physics, for providing the facilities for AFM measurements. We also thank Mr Jaakko Niinistö M.Sc. (Eng.), for the AFM measurements.

## References

1 P. J. Martin, H. A. Macleod, R. P. Netterfield, C. G. Pacey and W. G. Sainty, *Appl. Opt.*, 1983, **22**, 178.
2 J. L. Deschanvres, J. M. Vaca and J. C. Joubert, *J. Phys. IV*, 1995, **C5**, C5-1029.
3 X. Aslanoglou, P. A. Assimakopoulos, C. Trapalis, G. Kordas, M. A. Karakassides and M. Pilakouta, *Nucl. Instrum. Methods Phys. Res. Sect. B*, 1996, **118**, 630.
4 V. Craciun, D. Craciun and I. W. Boyd, *Electron. Lett.*, 1998, **34**, 1527.
5 A. Grafov, E. Mazurenko, G. A. Battiston and P. Zanella, *J. Phys. IV*, 1995, **C5**, C5-497.
6 M. Balog, M. Schieber, M. Michman and S. Patai, *Thin Solid Films*, 1977, **47**, 109.
7 H. Treichel, A. Mitwalsky, G. Tempel, G. Zorn, D. A. Bohling, K. R. Coyle, B. S. Felker, M. George, W. Kern, A. P. Lane and N. P. Sandler, *Adv. Mater. Opt. Electron.*, 1995, **5**, 163.
8 G. D. Wilk, R. M. Wallace and J. M. Anthony, *J. Appl. Phys.*, 2001, **89**, 5243.
9 Y. Ma, Y. Ono, L. Stecker, D. R. Evans and S. T. Hsu, *Tech. Dig. Int. Electron Devices Meet.*, 1999, 149.
10 Y. Komatsu, T. Sato, S. Ito and K. Akashi, *Thin Solid Films*, 1999, **341**, 132.
11 Y. Yu, X. Wang, Y. Cao and X. Hu, *Appl. Surf. Sci.*, 2001, **172**, 260.
12 T. Kim, J. Oh, B. Park and K. S. Hong, *Jpn. J. Appl. Phys.*, 2000, **39**, 4153.
13 F. F. Lange, *J. Mater. Sci.*, 1982, **17**, 225.
14 E. N. Farabaugh, A. Feldman, J. Sun and Y. N. Sun, *J. Vac. Sci. Technol. A*, 1987, **5**, 1671.
15 F. Tcheliebou, M. Boulouz and A. Boyer, *J. Mater. Res.*, 1997, **12**, 3260.
16 S. B. Quadri, E. F. Skelton, M. Harford, P. Lubitz and L. Aprigliano, *J. Vac. Sci. Technol. A*, 1990, **8**, 2344.
17 F. Hanus and L. D. Laude, *Appl. Surf. Sci.*, 1998, **127–129**, 544.
18 R. D. Maggio, A. Tomasi and P. Scardi, *Mater. Lett.*, 1997, **31**, 345.
19 A. Galtayries, M. Crucifix, G. Blanchard, G. Terwagne and R. Sporken, *Appl. Surf. Sci.*, 1999, **142**, 159.
20 A. N. Khodan, J.-P. Contour, D. Michel, O. Durand, R. Lyonnet and M. Mihet, *J. Cryst. Growth*, 2000, **209**, 828.
21 S. B. Qadri, H. R. Khan, E. F. Skelton and P. Lubitz, *Surf. Coat. Technol.*, 1998, **100–101**, 94.
22 A. Nazeri and S. B. Qadri, *Surf. Coat. Technol.*, 1996, **86–87**, 166.
23 Y. Takahashi, T. Kawae and M. Nasu, *J. Cryst. Growth*, 1986, **74**, 409.
24 G. Garcia, J. Casado, J. Llibre and A. Figueras, *J. Gryst. Growth.*, 1995, **156**, 426.
25 C. Dubordieu, S. B. Kang, Y. Q. Li, G. Kulesha and B. Gallois, *Thin Solid Films*, 1999, **339**, 165.
26 M. Putkonen, T. Sajavaara, J. Niinistö, L.-S. Johansson and L. Niinistö, *J. Mater. Chem.*, submitted.
27 J. Qiao and C. Y. Yang, *Mater. Sci. Eng.*, 1995, **R14**, 157.
28 Y. J. Tian, S. Linzen, F. Schmidl, A. Matthes, H. Schneidewind and P. Seidel, *Thin Solid Films*, 1999, **338**, 224.
29 W. Prusseit, S. Corsépius, M. Zwerger, P. Berberich, H. Kinder, O. Eibl, C. Jaekel, U. Breuer and H. Kurz, *Physica C*, 1992, **201**, 249.
30 G. Garcia, A. Figueras, J. Casado, J. Llibre, M. Mokchah, G. Petot-Ervas and J. Calderer, *Thin Solid Films*, 1998, **317**, 241.
31 G.-L. Tan and X.-J. Wu, *Thin Solid Films*, 1998, **330**, 59.
32 K.-W. Chour, J. Chen and R. Xu, *Thin Solid Films*, 1997, **304**, 106.
33 J. Han, G. Xomeritakis and Y. S. Lin, *Solid State Ionics*, 1997, **93**, 263.
34 C.-H. Lin, W.-D. Hsu and I.-N. Lin, *Appl. Surf. Sci.*, 1999, **142**, 418.
35 T. Shiosaki, H. Fujisawa and M. Shimizu, *Proc. IEEE Int. Symp. Appl. Ferroelectr.*, 1996, 45.
36 J. F. Scott and C. A. Paz De Araujo, *Science*, 1989, **246**, 1400.
37 T. S. Suntola, A. J. Pakkala and S. G. Lindfors, *US Pat.*, 4 413 022, 1983.
38 L. Niinistö, M. Ritala and M. Leskelä, *Mater. Sci. Eng. B*, 1996, **41**, 23.
39 L. Niinistö, *Curr. Opin. Solid State Mater. Sci.*, 1998, **3**, 147.
40 L. Niinistö, *Proc. Int. Semicond. Conf.*, 2000, 33.
41 T. Suntola, *Handbook of Thin Film Process Technology*, ed. D. A. Glocker and S. I. Shah, Institute of Physics, Bristol, 1995, pp. B1.5 1–17.
42 M. Ritala and M. Leskelä, *Appl. Surf. Sci.*, 1994, **75**, 333.
43 K. Kukli, M. Ritala and M. Leskelä, *Chem. Vap. Deposit.*, 2000, **6**, 297.
44 M. Copel, M. Gribelyuk and E. Gusev, *Appl. Phys. Lett.*, 2000, **76**, 436.
45 E. P. Gusev, M. Copel, E. Cartier, D. Buchanan, H. Okorn-Schmidt, M. Gribelyuk, D. Falcon, R. Murphy, S. Molis, I. J. R. Baumvol, C. Krug, M. Jussila, M. Tuominen and S. Haukka, *Proc. Electrochem. Soc.*, 2000, **2**, 477.
46 A. Kytökivi, E.-L. Lakomaa, A. Root, H. Österholm, J.-P. Jacobs and H. H. Brongersma, *Langmuir*, 1997, **13**, 2717.
47 M. Kröger-Laukkanen, M. Peussa, M. Leskelä and L. Niinistö, *Appl. Surf. Sci.*, in press.
48 J. Gavillet, T. Belmonte, D. Hertz and H. Michel, *Thin Solid Films*, 1997, **301**, 35.
49 D. G. Colombo, D. C. Gilmer, V. G. Young Jr., S. A. Campbell and W. L. Gladfelter, *Chem. Vap. Deposit.*, 1998, **4**, 220.
50 J. Si, S. B. Desu and C.-Y. Tsai, *J. Mater. Res.*, 1994, **9**, 1721.
51 M. A. Cameron and S. M. George, *Thin Solid Films*, 1999, **348**, 90.
52 J. J. Gallegos III, T. L. Ward, T. J. Boyle, M. A. Rodriguez and L. P. Francisco, *Chem. Vap. Deposit.*, 2000, **6**, 21.
53 A. C. Jones, T. J. Leedham, P. J. Wright, M. J. Crosbie,

D. J. Williams, K. A. Fleeting, H. O. Davies, D. J. Otway and P. O'Brien, *Chem. Vap. Deposit.*, 1998, **4**, 197.
54 M. Morstein, I. Pozsgai and N. D. Spencer, *Chem. Vap. Deposit.*, 1999, **5**, 151.
55 M. Morstein, *Inorg. Chem.*, 1999, **38**, 125.
56 A. Bastianini, G. A. Battiston, R. Gerbasi, M. Porchia and S. Daolio, *J. Phys. IV*, 1995, **C5**, C5-525.
57 S. Codato, G. Carta, G. Rossetto, G. A. Rizzi, P. Zanella, P. Scardi and M. Leoni, *Chem. Vap. Deposit.*, 1999, **5**, 159.
58 L. M. Dyagileva and E. I. Tsyganova, *Zh. Obshch. Khim.*, 1995, **65**, 1057; L. M. Dyagileva and E. I. Tsyganova, *Russ. J. Gen. Chem. (Engl. Transl.)*, 1995, **65**, 963.
59 M. Leskelä and M. Ritala, *J. Phys. IV*, 1999, **9**, Pr8–837.
60 A. W. Ott, K. C. McCarley, J. W. Klaus, J. D. Way and S. M. George, *Appl. Surf. Sci.*, 1996, **107**, 128.
61 M. Putkonen, T. Sajavaara and L. Niinistö, *J. Mater. Chem.*, 2000, **10**, 1857.
62 M. Vehkamäki, T. Hatanpää, T. Hänninen, M. Ritala and M. Leskelä, *Electrochem. Solid State Lett.*, 1999, **2**, 504.
63 E. Samuel and M. D. Rausch, *J. Am. Chem. Soc.*, 1973, **95**, 6263.
64 N. B. Morozova, I. K. Igumenov, V. N. Mit'kin, K. V. Kradenov, O. G. Potapova, V. B. Lazarev and Ya. Kh. Grinberg, *Zh. Neorg. Khim.*, 1989, **34**, 1193; N. B. Morozova, I. K. Igumenov, V. N. Mit'kin, K. V. Kradenov, O. G. Potapova, V. B. Lazarev and Ya. Kh. Grinberg, *Russ. J. Inorg. Chem. (Engl. Transl.)*, 1995, **65**, 963.
65 M. Leskelä, L. Niinistö, E. Nykänen, P. Soininen and M. Tiitta, *Thermochim. Acta*, 1991, **175**, 91.
66 M. Ylilammi and T. Ranta-aho, *Thin Solid Films*, 1993, **232**, 56.
67 *UniQuant Version 2 User Manual*, Omega Data Systems, Veldhoven, Netherlands, 1994.
68 J. Jokinen, J. Keinonen, P. Tikkanen, A. Kuronen, T. Ahlgren and K. Nordlund, *Nucl. Instrum. Methods Phys. Res., Sect. B*, 1996, **119**, 533.
69 M. Putkonen, T. Sajavaara, L.-S. Johansson and L. Niinistö, *Chem Vap. Deposit.*, 2001, **7**, 44.
70 M. Nieminen, M. Putkonen and L. Niinistö, *Appl. Surf. Sci.*, 2001, **174**, 155.
71 E. Wisotzki, A. G. Balogh, H. Hahn, J. T. Wolan and G. B. Hoflund, *J. Vac. Sci. Technol. A*, 1999, **17**, 14.
72 R. Suyama, T. Ashida and S. Kume, *J. Am. Ceram. Soc.*, 1985, **68**, C314.
73 J. Aarik, A. Aidla, T. Uustare and V. Sammelselg, *J. Cryst. Growth*, 1995, **148**, 268.
74 J. Aarik, A. Aidla, A.-A. Kiisler, T. Uustare and V. Sammelselg, *Thin Solid Films*, 1999, **340**, 110.